Chalmers Publication Library

Benefit of Route Recognition in Energy Management of Plug-in Hybrid Electric Vehicles

(article starts on next page)

Benefit of Route Recognition in Energy Management of Plug-in Hybrid Electric Vehicles

Viktor Larsson[a], Lars Johannesson[a,b], Bo Egardt[a] and Anders Lassson[c]

Abstract— **This paper investigates the benefit of an energy management system that autonomously can recognize when a plug-in hybrid electric vehicle is driven along known commuting routes. The presented route recognition algorithm compares the GPS trajectory of the ongoing trip with stored commuting routes using the well known cross-correlation operation. If a route is recognized the energy management system switches from a charge depleting charge sustaining discharge strategy to a strategy where the battery discharge rate is adapted to the length of the recognized route, thereby decreasing the average discharge current and the resistive losses.**

The proposed system is evaluated using simulations on one month of logged commuter driving data. The results for an energy management system based on the equivalent consumption minimization strategy indicate an overall fuel cost reduction of 1.5% compared to an system that only utilize a charge depleting charge sustaining strategy.

I. INTRODUCTION

At the present day the automotive industry is undergoing an electrification process to counter the challenges posed by global warming and the expected peak in oil production. Due to the high cost of battery capacity, the electrification was until a few years ago limited to Hybrid Electric Vehicles (HEVs) with an electric range of at most a few kilometers.

However, recent advances in battery technology has lowered battery cost significantly, thus indicating that the next major step in the electrification will be the introduction of Plug-in Hybrid Electric Vehicles (PHEVs) to the mass market. A PHEV has a high capacity battery, which can be charged through the electric grid, thereby providing an All Electric Range (AER) of at least 10 km; for example the rated AER of the 2012 plug-in Prius is about 18 km [1].

One potential target group for PHEVs is arguably individuals that commute longer distances to and from work on a daily basis. In Sweden 11% of the labor force commuted longer than 30 km to work (median distance 50 km) in the year 2000 [2]. Hence, it is likely that a large fraction of PHEV commuters might drive a distance exceeding the AER during a commuting trip (a trip is defined as the driving between two consecutive charging occasions), especially if they do not charge at work.

For trips exceeding the AER there is a degree of freedom concerning the discharge rate of the battery. How this degree of freedom should be exploited by the Energy Management System (EMS) has been investigated in [3]–[6]. The studies compare the trivial Charge Depleting - Charge Sustaining

(CDCS) strategy with blended strategies, i.e. strategies that continuously blend battery energy with fuel energy such that the battery is depleted at the very end of the trip. A blended strategy lowers the electric losses mainly by: i) lowering the average battery current and ii) avoiding that the ICE is used to charge the battery during CS operation. Results show that a blended strategy can reduce the fuel consumption with up to 20% compared to the CDCS strategy [4]. However, the results in [3]–[5] indicate that the fuel cost reductions are highly dependent on trip length and vehicle configuration, with higher reductions possible for trip lengths somewhat longer than the AER and PHEVs with low efficiency in CS mode (e.g. PHEVs with high power ICE's).

The main disadvantage of a blended strategy is the need for accurate a priori information regarding the future trip. If the prediction is poor the discharge rate might be to slow and the trip could end with a partially discharged battery, implying that with increasing uncertainty the fuel cost might increase rather than decrease. Earlier studies have considered situations where the future trip is known either perfectly, [5], or partly a priori, [3], [4], [7]. However, a priori information is typically only available when the driver explicitly has informed the vehicle of the coming trip through the navigation system, a scenario which might be considered unrealistic for every day usage due to the extra effort required. A more convenient approach would be to let the vehicle autonomously recognize trips going along commuting routes and thereby acquire a priori information regarding the future trip, something that was investigated for more general automotive applications in [8]. Previous studies related to energy management and autonomous recognition have primarily been focused on HEVs and on driving pattern recognition, i.e. to recognize suburban, highway or congested driving, and not considered recognition of individual routes, see for example [9], [10].

Recognizing a lack of studies concerning blended strategies and route recognition, the aim of this paper is twofold. First and foremost, the paper presents an EMS with route recognition. A novel heuristic route recognition algorithm is proposed based on the trip GPS-trajectory and starting time. If the ongoing trip is recognized the EMS switches from a CDCS strategy to a blended strategy where the battery State of Charge (SoC) reference is decreased linearly with the remaining route distance. The power split controller used to follow the SoC reference is based on the well known Equivalent Consumption Minimization Strategy (ECMS), see [9], [11]. The main benefit of the proposed route recognition algorithm is its relatively low complexity and ease of im-

[a]Department of Signals & Systems, Chalmers University of Technology, Gothenburg Sweden, e-mail: {lviktor, larsjo, egardt}@chalmers.se

[b]Viktoria Institute, e-mail: lars.johannesson@viktoria.se

[c]Volvo Car Corporation, e-mail: alasson@volvocars.com

plementation due to not relying on a digital map. Secondly, the paper evaluates the proposed EMS in a case study with simulations on one month of logged driving data for a family with a commuting driving pattern. A real driving pattern is necessary for a fair comparison of the overall fuel costs between the proposed EMS and the trivial CDCS strategy, used when no a priori information is available.

A. Paper Outline

The paper is divided into seven sections. After the introduction the proposed EMS is introduced and the power split control strategy used to follow the SoC reference is explained. Succeeding sections covers the logged commuter driving data and the simulation study. The paper is ended with discussion and conclusions and an appendix describing the vehicle model and parts of the route recognition algorithm.

II. AN EMS WITH ROUTE RECOGNITION

The proposed EMS with integrated route recognition is divided into three separate parts, each of them outlined below.

A. Data Collection and Route Clustering

The vehicle should continuously collect, store and cluster driving data such as: velocities, GPS-positions and trip starting times. The clustering problem is however beyond the scope of this paper and is therefore not considered further. During the reminder of the paper the EMS is assumed to have access to already structured route data.

The identified commuting routes, $i = 1, 2, ..., p$, are represented by the data structure shown in Table I, specifying the expected GPS-position of the vehicle as a function of the distance travelled since the start of the route. Furthermore, the data structure also contains information regarding the mean route: length, starting time and energy demand at the wheels, with associated standard deviations.

TABLE I

THE DATA STRUCTURE CHARACTERZING A ROUTE, i.

Data Type	Symbol	Unit
Index	k	1,2,...,N
Distance	z_k	km
Latitude, Longitude	x_k, y_k	dec.
Start Time, Mean / Std	$\bar{t}_0$, σ_{t_0}	hh:mm:ss
Route Length, Mean / Std	$\bar{z}$, σ_z	km
Route Energy, Mean / Std	$\bar{E}_N$, σ_{E_N}	MJ

B. Route Recognition Algorithm

The algorithm can be summarized as follows:

1) Initialization: At the start of the trip determine the initial GPS-position of the vehicle and the start time. All commuting routes with initial positions and start times within d^* km and T^* minutes are designated possible candidate routes.

2) Real-Time Loop: While driving calculate the normalized 2-dimensional cross-correlation between the currently logged GPS-trajectory and the trajectories of the candidate routes. From the obtained matrices determine the route, i^*, with the highest cross-correlation value, s^*, and the corresponding position offset, Δz^*, i.e. the distance lag between the two coordinate trajectories. The whole procedure is described in detail in Appendix I.

3) Recognition Criterion: The current trip is positively matched against a candidate route, at sample k, if s_k^* is greater than the threshold s_{lim} and the travelled distance, z_k, exceeds the threshold distance z_o. The condition on the travelled distance is added to avoid false matching when the data set is small, i.e. early on in a trip. If several of the candidate routes satisfy these criterions the shortest candidate route is chosen as the matching route.

C. EMS Modes

The EMS operates in two modes, separating whether or not the current trip has been recognized as a route.

1) The CDCS Mode: The default mode used when no route has been recognized, consequently there is no information available regarding the future driving and the trip could end at any moment. To minimize the expected energy cost the PHEV should operate in charge depletion mode until the battery is depleted and then proceed in charge sustaining operation. Hence, the SoC reference is set to the lower limit, i.e. $SoC_{\text{ref}}(t) = SoC_{\text{f}}$.

2) The Blended Mode: If the current trip is recognized as a commuting route, the EMS switches to a blended discharge strategy. In this paper the topography is assumed flat and the SoC reference is therefore simply decreased linearly with the remaining route distance, an approach shown to give close to optimal results on flat topography [6], [7]. Denote the time when the trip is recognized as a commuting route t^*, from that time the SoC reference is given by

$$SoC_{\text{ref}}(t) = SoC(t^*) - \tag{1}$$
$$\min\left\{1, \frac{z_c(t) - z_c(t^*)}{\hat{z} - z_c(t^*)}\right\}(SoC_{\text{f}} - SoC(t^*)),$$

where SoC_{f} is the lower SoC limit. The corrected vehicle distance position along the route, i.e. compensated for the distance lag between the trip and the identified route, is given by $z_c(t) = z(t) + \Delta z^*(t)$. Furthermore, to avoid an overestimation of the trip length and the possibility that the trip ends with only a partially discharged battery, the trip length prediction is set to: $\hat{z} = \bar{z} - 2\sigma_z$, meaning that only about 2.3% of the trips recognized will have overestimated trip lengths, provided that the expected trip length is a normally distributed unbiased estimate.

III. POWER SPLIT CONTROL STRATEGY

The well known ECMS strategy, see [9], [11], is used in both EMS modes to follow the SoC reference. The main idea in ECMS can be summarized as to find the control signal, u, that minimize the cost function

$$J(t, u) = \dot{m}_{\text{f}}(t, u) \cdot H_{\text{LHV}} + s(t) \cdot P_{\text{bat}}(t, u), \tag{2}$$

where $\dot{m}_f$ represents the fuel mass rate of the ICE, H_{LHV} the lower heating value of the fuel used and P_{bat} the battery power (defined positive during discharge). The control signal u determines the power split between the ICE and the battery and the variable $s(t)$ represents the equivalence factor translating battery energy into an equivalent fuel energy.

For each specific trip there exists an equivalence factor, s, that yields the desired final SoC on that trip. However, in practice a trip is never known a priori and the correct equivalence factor remains unknown. This paper will utilize the following approximate expression for the equivalence factor

$$s(t) = p(t) \cdot s_{dis} + (1 - p(t)) \cdot s_{chg}, \tag{3}$$

originally proposed in [11], where s_{dis} is the value of the equivalence factor that results in electric vehicle mode and s_{chg} is the value that leads to ICE based traction combined with charging of the battery, see [11] for a detailed description of how these parameters are defined and determined.

The weighting variable $p(t)$ governs the discharge rate of the battery and is given by

$$p(t) = \frac{s_{dis}}{s_{dis} + s_{chg}} + \frac{E_e(t) - E_{ref}(t) - \lambda E_r(t)}{E_r(t)} \frac{\sqrt{s_{dis} s_{chg}}}{s_{dis} + s_{chg}}, \tag{4}$$

where $p(t)$ is truncated such that $p(t) \, \epsilon \, [0, 1]$. Furthermore, $E_r(t)$ represents the expected remaining energy demand of the trip at time t, λ represents the fraction of the energy delivered to the wheels that can be recuperated by the electrical path and $E_e(t)$ corresponds to the battery energy consumed up to time t.

For an HEV no net depletion of the battery is desired and the reference for the net change in battery energy, $E_{ref}(t)$, is typically zero. However, this is not the case for a PHEV where the battery should be depleted. Hence

$$E_{ref}(t) = (SoC_0 - SoC_{ref}(t)) \cdot E_{bat}, \tag{5}$$

where E_{bat} represents the nominal energy stored in the battery and SoC_0 the initial battery SoC.

IV. Logged Commuter Driving Data

The authors were given access to logged driving data from a joint PHEV demonstration project [12] carried out by the Swedish power company Vattenfall AB, ETC Battery and FuelCells Sweden AB and Volvo Car Corporation. During one year all the driving of two test vehicles were logged; each vehicle was driven for approximately one month by one family before it was passed on to a new family. The logged data used in this paper is the vehicle velocity, GPS-position and trip starting time. The altitude was not logged and is for simplicity assumed to be constant throughout the paper.

The logged driving pattern for one of the participating families is shown in Figure 1. The upper left plot depicts a histogram of the trip lengths and the upper right plot shows the corresponding GPS trajectories. During the logging period of one month this family drove 1834 km dispersed on 120 trips ranging from 0.1 km to 225 km. The histogram shows a clear peak at a trip length of approximately 33 km, indicating the commuting route(s), also seen as the thick solid line among the GPS-trajectories in the right plot. Worth to note is that 44 % of the total driving, for this family, is along the commuting route(s), i.e. 805 km out of the total 1834 km. Denote the starting and ending positions of the commuting route(s) *home* and *work* respectively. Figure 2 depicts the GPS and velocity trajectories of the trips starting either at *home* or at *work*. The figure clearly shows that there are two slightly alternate paths, *a* and *b*, going between *home* and *work*.

Furthermore, some of the trips driven share the same initial path as the commuting route(s) but have different final destinations, meaning that the GPS-trajectory alone is not enough to unambiguously identify a trip driving along a commuting route, at least early on during the trip. Note however, that all the commuting trips have isolated start times with low variability, as seen in the lower plots of Figure 1 that depicts scatter plots of the start times vs. trip lengths for the trips starting at *home* and *work*. Finally, the statistics for the commuting trips are summarized in Table II.

TABLE II
STATISTICS FOR THE COMMUTING TRIPS.

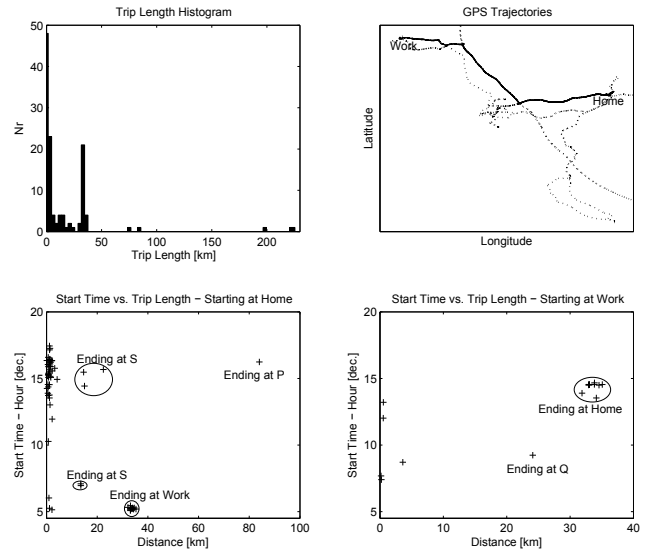| Path	Nr	Length [km]	Start Time [hh:mm:ss]	Energy [MJ]
		$\bar{z}$ (σ_z)	$\bar{t}_0$ (σ_{t_0})	$\bar{E}_N$ (σ_{E_N})
Home-Work	13	33.6 (0.8)	05:14:07 (05:21)	15.2 (1.2)
Work-Home	11	33.5 (0.9)	14:23:47 (20:55)	16.0 (0.7)
Both dir.	24	33.6 (0.8)	-	15.6 (1.1)

Fig. 1. The upper plots shows the trip length histogram, left, and the corresponding GPS trajectories, right. The lower plots shows scatter plots of the start times vs. trip lengths for the trips starting at *home* and *work*.
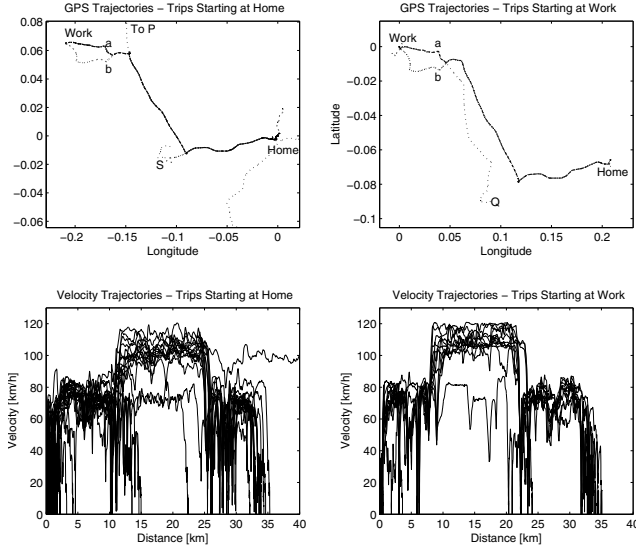
Fig. 2. The upper plots shows the GPS trajectories of the trips starting at *home*, left, and *work*, right. The lower plots depicts the corresponding velocity trajectories.

V. SIMULATION STUDY USING LOGGED DRIVING DATA

The simulation study is performed using the logged commuter driving data described in Section IV and the benefit of the proposed EMS is evaluated by comparing it to a nominal EMS that does not use route recognition, i.e. uses the CDCS mode at all times.

The PHEV model used during the simulations is a parallel hybrid with an Electric Machine (EM) driving the rear axle and a Spark Ignited (SI) ICE driving the front axle and a small generator that can be used to charge the battery. The battery is of Li-Ion type and provides an AER of approximately 15-25 km depending on the driving conditions. See Appendix II for a more detailed description of the vehicle model.

Three performance measures are used to compare the two EMS's: i) the fuel cost (gasoline and electricity), ii) the fuel consumed (gasoline) and iii) the battery Ah throughput. The Ah throughput is of relevance since it is correlated with battery wear, see [13]. The gasoline and electricity prices used are 1.61 €/liter and 0.10 €/kWh. Furthermore, it is assumed that the efficiency when charging the battery at the end of the trip is 90 percent.

A. Simulation Setup

From the logged driving data four commuting routes were identified: 1_a, 1_b, 2_a and 2_b; where $1, 2$ separates routes going between *home-work* and *work-home* respectively. The two slightly different paths possible for each driving direction are distinguished by index a, b as seen in Figure 2. The GPS-trajectories of the routes are defined by one of the logged trips along that route.

All the 120 logged trips from Section IV were simulated with both the nominal and the proposed EMS, under the assumption that the battery is fully recharged after each

trip, i.e. up to SoC_0. For simplicity all four commuting routes use the same parameters and route statistics, except starting times, shown in Table III. Furthermore, to have a fair comparison of the the nominal and the proposed EMS, both strategies use the mean values of the ECMS parameters obtained on the commuting routes. Note that due to the limited data set, one month of logged data, the training data used to identify the route parameters/statistics is the same as the simulation data. Finally, to give an idea of the performance the results are also compared to the optimal discharge strategy determined using Dynamic Programming (DP) [14].

TABLE III
THE PARAMETER VALUES USED DURING THE SIMULATIONS.

Route Rec. Par.		
T^*	60 [min]	
d^*	3 [km]	
z_0	3 [km]	
$s_{\lim}$	0.995	
Route Stat.	$i = 1_a, 1_b, 2_a, 2_b$	
$\bar{z}^i$ (σ_z^i)	33.6 (0.8) [km]	
$\bar{E}_N^i$ $(\sigma_{E_N}^i)$	15.6 (1.1) [MJ]	
$\bar{t}_0^1$, $\bar{t}_0^2$	05:14:07, 14:23:47	
EMS Par.	**CDCS Mode**	**Blended Mode**
$E_r(t)$	0.25 [MJ]	$\bar{E}_N^i - 2\sigma_{E_N}^i$ $- \int_{t_o}^t \tau_{wh}(s)\omega_{wh}(s)ds$
$SoC_{\mathrm{ref}}(t)$	SoC_f	Eq. (1)
ECMS Par.	**Commuting Route Mean** (std)	
s_{dis}	3.92 (0.14)	
s_{chg}	2.29 (0.07)	
λ	0.03 (0.02)	

B. Simulation Results

Simulation results for one of the commuting trips, *Trip A* starting at *home* at 05:13:19 and following route 1_a, are depicted in Figure 3. The figure show that the proposed EMS identifies both route 1_a and 1_b as candidate routes for *Trip A*, since both these routes starts at *home* with mean starting time 05:14:07. The maximum cross-correlation, s^*, between *Trip A* and the candidate routes is very close to unity for both routes since they follow the same path during most of the way. However, there is a notable difference near the end of the trip, due to the slightly different paths of the candidate routes when approaching the final destination, *work*. From the figure it is clear that the proposed EMS results in a blended discharge strategy with a SoC trajectory lying relatively close to the optimal SoC trajectory determined using DP; this in contrast to the nominal EMS where the battery is depleted about halfway into the trip.

Similar results are shown in Figure 4 which depicts the simulation results obtained on another commuting trip, *Trip B*, starting at *work* at 14:33:09 and going along route 2_a. Note that for this example, the cross-correlation between *Trip B* and the candidate routes, 2_a and 2_b, exhibit a slightly different behavior since the candidate routes follow slightly different paths during the beginning rather than the end of the route.
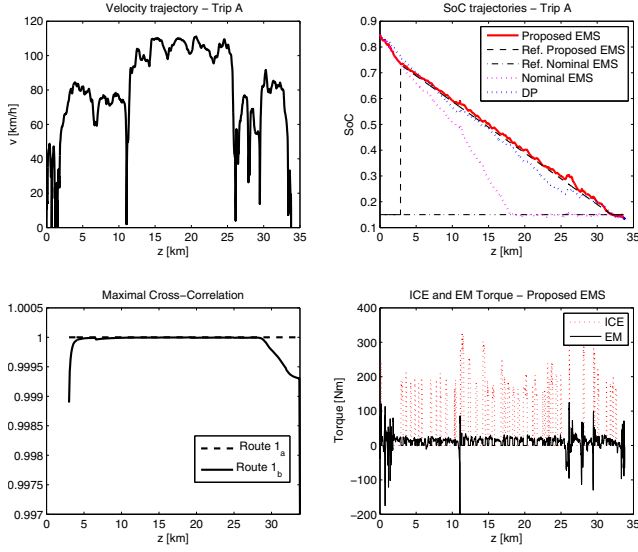
Fig. 3. Simulation of a commuting trip, *Trip A*, along route 1_a. The upper plots show the trip velocity trajectory and the SoC trajectories for the nominal and the proposed EMS. The lower plots depicts the maximal cross-correlation between the trip and the candidate routes and the torques of the ICE and the EM for the proposed EMS.
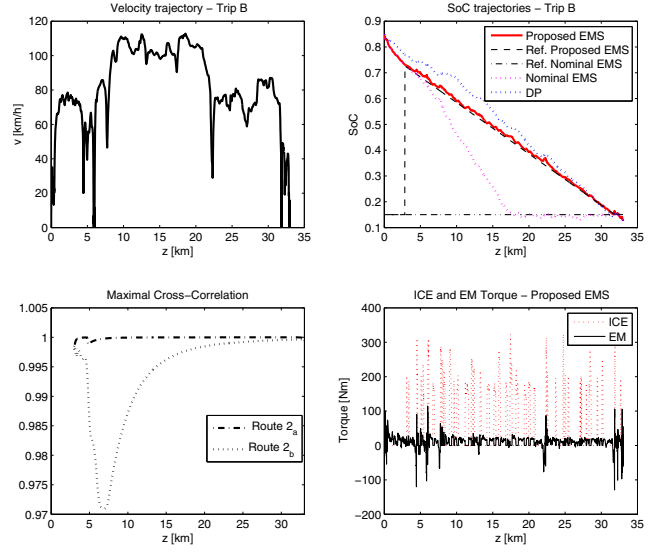

Fig. 4. Simulation of a commuting trip, *Trip B*, along route 2_a. The upper plots show the trip velocity trajectory and the SoC trajectories for the nominal and the proposed EMS. The lower plots depicts the maximal cross-correlation between the trip and the candidate routes and the torques of the ICE and the EM for the proposed EMS.

Table IV shows the fuel costs and the final SoC values obtained for *Trip A* and *Trip B*. The table indicates that the proposed EMS achieves fuel costs close to optimality, thereby reducing the fuel costs with 3.1% (*Trip A*) and 5.8% (*Trip B*) compared to the nominal EMS. Furthermore, Table V summarizes the overall fuel costs, fuel consumption and battery Ah throughput obtained during the simulations; both for the 24 logged commuting trips and for all the 120 trips made during the logging period (i.e. both commuting and non-commuting trips). For the investigated logging period the proposed EMS will result in: 1.5% lower fuel cost, 1.9% lower fuel consumption and 3.8% lower Ah throughput compared the nominal EMS.

VI. DISCUSSION

The simulations illustrate the importance of evaluating the usage of blended strategies on realistic driving patterns. For individual trips the fuel cost can be reduced significantly, more than 6%. However, since some fraction of the trips made with a PHEV will be shorter than the AER, the overall fuel cost savings will be lower.

The benefit of the proposed EMS will to a large extent depend on the driving pattern of the PHEV; a driver that rarely drives trips exceeding the AER will have practically no benefit of the proposed EMS. However, a long distance commuter driving a significant fraction of the total distance along well known routes, exceeding the AER, will likely have a notable fuel cost reduction. Furthermore, the benefit of a blended strategy is closely connected to the resistive losses in the electrical path, thus meaning that the benefit will improve with increased battery resistance, i.e. with battery aging and at low battery temperatures. Also worth to point out is that the proposed route recognition method is not dependent on digital map data but only on having access to the GPS position and the calendar time, meaning that software integration and licensing issues can be avoided.

Although the simulation results are promising for the studied family, the route recognition can be improved further, for example by including: average route speed, weekday, allowing different starting times for the same route (e.g. people working shift), etc. The proposed technique could also be compared with more sophisticated methods such as Hidden Markov Models, as proposed in [15], or Support Vector Regression.

TABLE IV

THE FUEL COST AND FINAL SOC VALUES OF TRIP A AND TRIP B.

Trip / Trips	Nominal EMS		Proposed EMS		DP	
	€	SoC_f	€	SoC_f	€	SoC_f
Trip A	1.95	0.131	1.89	0.133	1.85	0.133
Trip B	1.91	0.121	1.80	0.126	1.77	0.125

TABLE V

THE FUEL COST, FUEL CONSUMPTION AND THE AH-THROUGHPUT OF THE NOMINAL EMS AND THE PROPOSED EMS.

Trip / Trips	Control Strategy					
	Nominal EMS			Proposed EMS		
	€	Fuel [kg]	Ah [MAh]	€	Fuel [kg]	Ah [MAh]
All com. trips	46.1	21.7	2.66	44.4	20.7	2.43
All trips	116.9	59.0	5.84	115.2	57.9	5.62

VII. Conclusion

The results obtained during the simulations indicate that for the logged commuting driving data used in this paper, the proposed EMS can give non negligible reductions in overall fuel costs, fuel consumption and battery Ah throughput. The reduced Ah throughput should reduce battery wear, see [13], although to what extent is uncertain. Furthermore, the fuel cost savings depends on the price ratio between fuel and electricity, if the price of gasoline increases the cost savings will be slightly higher. However, further research and experimental tests are needed to verify the results and determine if similar figures are possible for other commuting patterns.

Appendix I
The Normalized 2-dimensional Cross-Correlation

The normalized 2-dimensional cross-correlation between the ongoing driving trajectory and the driving trajectory of a candidate route is calculated using the image processing procedure proposed in [16]. Although, here the usage is slightly different compared to conventional template matching, rather than interpreting the two driving trajectories as sliding images they are interpreted as two dimensional vectors of real numbers (the GPS coordinates) that slide along one another.

The expression for the 2-dimensional cross-correlation is given by

$$\gamma_k^i(u,v) = \tag{6}$$
$$\frac{\sum_{x,y} \left[f^i(x,y) - \bar{f}_{u,v}^i\right]\left[t_k(x-u,y-v) - \bar{t}_k\right]}{\sqrt{\sum_{x,y}\left[f^i(x,y) - \bar{f}_{u,v}^i\right]^2 \sum_{x,y}\left[t_k(x-u,y-v) - \bar{t}_k\right]^2}}.$$

Where $f^i(x,y)$ is the image, i.e. the GPS-coordinate vector of the candidate route of comparison, $f^i(x,y) = [x_{1:N}^i - x_o, \ y_{1:N}^i - y_o] \in \mathbb{R}^{N \times 2}$ and $t_k(x,y)$ is the template, i.e. the GPS-coordinate vector of the ongoing driving trajectory at the current sample k, $t_k(x,y) = [x_{1:k} - x_o, \ y_{1:k} - y_o] \in \mathbb{R}^{k \times 2}$. The coordinates of both the template and the image, f and t, are taken with respect to the starting position of the ongoing trip to remove bias effects, i.e. cross-correlations very close to unity. Furthermore, $\bar{t}_k$ represents the mean of the template and $\bar{f}_{u,v}$ represents the mean of the image in the region under the template.

From the resulting cross-correlation matrix, $\gamma_k^i(u,v) \in \mathbb{R}^{(N+k-1)\times 3}$, the highest cross-correlation value is $s_k^{*,i} = \max_u \gamma_k^i(u,2)$ and the corresponding position offset is $\Delta z_k^{*,i} = \delta z \cdot (argmax_u \ \gamma_k^i(u,2) - k)$, where δz is spatial resolution.

Appendix II
Vehicle Model

The vehicle configuration used during the simulations is depicted schematically in Figure 5 and the vehicle parameters are summarized in Table VI. The powertrain is modeled using a quasi static approach, see [17], meaning that the mass fuel rate of the ICE, $\dot{m}_f(\omega_{ice}, \tau_{ice})$, and the losses in the EM/generator, $P_{loss}(\omega, \tau)$, are determined by linear interpolation between steady state measurements. The internal moments of inertia for the ICE, EM and generator are neglected and temperature effects are not considered for any part of the vehicle.

The torque required at the wheels, τ_{wh}, to follow the velocity trajectory of a trip can be determined using an inverse simulation approach [17] as

$$\tau_{wh} = r_{wh}(0.5 \cdot \rho_{air}C_dAv^2 + f_r mg + m\dot{v}), \tag{7}$$

where v represents the vehicle velocity and the road slope is assumed to be zero. The required torque must be met by the torque contributions from the EM, τ_{em}, the outgoing transmission torque, τ_{gb}, and the torque from the mechanical brakes, τ_{fr},

$$\tau_{wh} = \eta_r r_r \tau_{em} + \eta_f r_f \tau_{gb} + \tau_{fr}. \tag{8}$$

Note that the torque of the EM is defined as negative when acting as a generator and then the rear axis efficiency becomes η_r^{-1}. Furthermore, the outgoing transmission torque is proportional to the sum of the ICE torque, τ_{ice}, and the (negative) charging torque, τ_{ch},

$$\tau_{gb} = (\tau_{ice} + \tau_{ch})\eta_{gb} \cdot r_{gb,i}, \quad \tau_{ice} \geq -\tau_{ch} \geq 0 \tag{9}$$

where the gear box ratios are represented by $r_{gb,i}$, $i = 1,...,5$. The relation between the generator torque, τ_{gen}, and the charging torque is

$$\tau_{gen} = \frac{\tau_{ch}\eta_{r,gen}}{r_{gen}}. \tag{10}$$

The generator, ICE and EM speeds are: $\omega_{gen} = \omega_{ice}r_{gen}$, $\omega_{ice} = \omega_{wh}r_f r_{gb,i}$ and $\omega_{em} = \omega_{wh}r_r$; where ω_{wh} represents the rotational speed of the wheels. The choice of gear, $r_{gb,i}$, is given by a look-up table constructed from the gear ratios and the ICE maximum torque curve, with an added hysteresis mode to avoid excessive gear shifting. The dynamics during the gearshift are neglected.

The battery is of Li-Ion type and is modeled as an equivalent circuit with a voltage source in series with an internal resistance. The open circuit voltage is assumed to be an affine function of the SoC, $V_{oc}(SoC)$, and the internal resistance, R_{in}, is assumed to be constant. The battery SoC dynamics are given by

$$\frac{dSoC}{dt} = -\frac{I}{Q}, \tag{11}$$

where Q represents battery capacity and the relationship between battery current, I, and power, P_{bat}, is

$$P_{bat} = V(SoC)I - RI_{in}^2. \tag{12}$$

Finally, the power that the battery must supply is given by

$$P_{bat} = \tau_{em}\omega_{em} + P_{loss,em}(\tau_{em}, \omega_{em}) \tag{13}$$
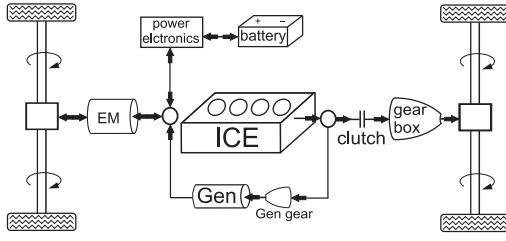$$+ \tau_{isg}\omega_{isg} + P_{loss,isg}(\tau_{isg}, \omega_{isg}) + P_{aux}.$$

Fig. 5. Schematic of the vehicle configuration, the arrows indicate the possible directions of power flow.

The control signal vector is: $u = [\tau_{em}, \ \tau_{ice}]^T$, where the generator torque is given implicitly by the torque split(s). Furthermore, if τ_{ice} is zero the ICE is considered to be off and $\dot{m}_f$ is zero. To prevent excessive ICE state transitions, turning on the ICE is penalized with a fuel equivalent, $m_{start} = g(\omega_{ice})$, which represents the fuel energy required to accelerate the ICE crankshaft to the required speed.

TABLE VI

VEHICLE DATA

Chassis Data	Symbol	Value
Mass, Wheel rad.	m, r_{wh}	1930 kg, 0.3m
Air / Roll. res.	$C_d A, f_r$	0.74, 0.012
Rear gear rat. / eff.	r_r, η_r	9.2, 0.965
Front gear rat. / eff.	r_f, η_f	3.1, 0.97
Gear box rat. / eff.	$r_{gb,i}, \eta_{gb}$	3.2, 2.0, 1.3, 0.9, 0.7; 0.97
Gen. gear rat. / eff.	$r_{gen}, \eta_{r,gen}$	2.7, 0.95
Aux. Power Demand	P_{aux}	1500 W
Battery Data		
Open cir. voltage	V_{oc}	202/181V@0.85/0.15 SoC
Resistance	R_{in}	0.10 Ω
Capacity	E_{bat}	5.9 kWh (4.1 usable)
SoC limits	SoC_o/SoC_f	0.85/0.15
SI ICE Data		
Max power	P_{max}	160 kW @ 5100 rpm
Max torque	τ_{max}	325 Nm @ 3000 rpm
EM Data		
Max power	P_{max}	50 kW
Max torque	τ_{max}	200 Nm up to 2100 rpm
Gen. Data		
Max power	P_{max}	21 kW
Max torque	τ_{max}	55 Nm up to 3500 rpm

APPENDIX III
ACKNOWLEDGMENTS

REFERENCES

[1] Toyota. [Online]. Available: http://www.toyota.com/prius-plug-in/
[2] E. Sandow and K. Westin, "The persevering commuter - Duration of long-distance commuting," *Transportation Research Part A: Policy and Practice*, vol. 44, no. 6, pp. 433–445, Jul. 2010.
[3] V. Larsson, L. Johannesson, and B. Egardt, "Impact of trip length uncertainty on optimal discharging strategies for PHEVs," in *Proceedings of the 6th IFAC AAC*, Munchen, 2010.
[4] D. Kum, H. Peng, and N. K. Bucknor, "Optimal Control of Plug-in HEVs for Fuel Economy Under Various Travel Distances," in *Proceedings of the 6th IFAC AAC*, Munchen, 2010.
[5] M. P. O. Keefe and T. Markel, "Dynamic Programming Applied to Investigate Energy Management Strategies for a Plug-in HEV," in *Proceedings of the 22nd International Battery, Hybrid and Fuel Cell Vehicle Symposium*, no. November, 2006.
[6] C. Zhang and A. Vahidi, "Route Preview in Energy Management of Plug-in Hybrid Vehicles," *IEEE Transactions on Control Systems Technology*, pp. 1–8, 2011.
[7] P. Tulpule, V. Marano, and G. Rizzoni, "Energy management for plug-in hybrid electric vehicles using equivalent consumption minimisation strategy," *Int. J. Electric and Hybrid Vehicles*, vol. 2, no. 4, 2010.
[8] J. Froehlich and J. Krumm, "Route Prediction from Trip Observations," in *Proceedings of SAE World Congress*, 2008.
[9] C. Musardo, G. Rizzoni, Y. Guezennec, and B. Staccia, "A-ECMS: An Adaptive Algorithm for Hybrid Electric Vehicle Energy Management," in *Proceedings of the 44th IEEE Conference on Decision and Control*, vol. 11, no. 4-5, Oct. 2005.
[10] S.-i. Jeon, S.-t. Jo, Y.-i. Park, and J.-m. Lee, "Multi-Mode Driving Control of a Parallel Hybrid Electric Vehicle Using Driving Pattern Recognition," *Journal of Dynamic Systems, Measurement, and Control*, vol. 124, no. 1, p. 141, 2002.
[11] A. Sciarretta, M. Back, and L. Guzzella, "Optimal Control of Parallel Hybrid Electric Vehicles," *IEEE Transactions on Control Systems Technology*, vol. 12, no. 3, pp. 352–363, May 2004.
[12] Vattenfall, "Att köra på el - Erfarenheter från Vattenfalls test av elfordon 2009-2010." [Online]. Available: http://newsroom.vattenfall.se/2010/07/07
[13] H. Wenzl, I. Baring-gould, R. Kaiser, B. Yann, P. Lundsager, J. Manwell, A. Ruddell, and V. Svoboda, "Life prediction of batteries for selecting the technically most suitable and cost effective battery," *Journal of Power Sources*, vol. 144, pp. 373–384, 2005.
[14] R. E. Bellman and S. E. Dreyfus, *Applied Dynamic Programming*. Princeton University Press, 1962.
[15] R. Simmons, B. Browning, and V. Sadekar, "Learning to Predict Driver Route and Destination Intent," in *Proceedings of the IEEE Intelligent Transportation Systems Conference*, 2006.
[16] J. P. Lewis, "Fast Normalized Cross-Correlation." [Online]. Available: http://www.idiom.com/~zilla/Papers/nvisionInterface/nip
[17] L. Guzzella and A. Sciarretta, *Vehicle Propulsion Systems*, 2nd ed. Berlin Heidelberg: Springer Verlag, 2007.